

## Article

# Multi-Time Interval Dynamic Optimization Model of New Energy Output Based on Multi-Energy Storage Coordination

Qiwei Wang<sup>1</sup>, Songqing Cheng<sup>1,\*</sup>, Shaohua Ma<sup>1</sup> and Zhe Chen<sup>1,2</sup><sup>1</sup> College of Electrical Engineering, Shenyang University of Technology, Shenyang 110870, China<sup>2</sup> The Faculty of Engineering and Science, Aalborg University, 9000 Aalborg, Denmark

\* Correspondence: chengsongqing@smail.sut.edu.cn

**Abstract:** In response to the problem of mismatch between new energy output and multi-energy load requirement in multi-energy power systems, this article proposes a dynamic optimization model for new energy output in multiple time intervals based on multi-energy storage coordination. First, considering the energy conversion characteristics of multi-energy storage, the dynamic optimization method of new energy output based on the discrete division of subinterval of scheduling time is studied. Then, considering the cost of adjusting various resources comprehensively, the optimization objective of new energy output is studied, and a model-solving method based on a directed graph topology distributed algorithm is proposed. Finally, simulation verification was conducted, and the simulation results showed that the method proposed in this paper can effectively suppress the new energy fluctuation and reduce peak-shaving costs.

**Keywords:** multi-energy storage; new energy; interval dynamic optimization; multi-time scale dispatch; distributed algorithm

## 1. Introduction

A multi-energy power system contains controllable primary energy input sources such as coal, gas, hydropower, and hydrogen energy. However, a multi-energy power system has strong randomness [1]. On the one hand, the access scale of new energy represented by wind and light is constantly increasing. On the other hand, the proportion of multi-energy loads dominated by traditional loads and new forms of loads such as heat and hydrogen are gradually increasing [2–5]. Therefore, the power and energy balance of multi-energy power systems at different spatial and temporal scales will be affected by the fluctuation of new energy power output and load, and will have a huge and extensive impact on the safe, stable, and economic operation of the multi-energy power system. In the multi-energy power system, the coordination of multi-energy storage and traditional flexibility regulation resources to optimize the output of new energy power generation with high efficiency and low cost is a new opportunity and challenge in the process of transformation from a traditional power system to a new power system [6].

The energy balance process of a multi-energy power system is complex, and many researchers have studied the energy balance problem of multi-energy power systems. Reference [7] established an optimal economic dispatch model to minimize the additional adjustment cost of multi-energy adjustable units, which reduced the congestion risk of multi-energy systems. Reference [8] proposed a multi-objective optimal scheduling method for multi-energy systems considering environmental costs, carbon transaction costs, and operating costs. Reference [9] proposed an electric-thermal hybrid power flow calculation method, which can intuitively express the electric, thermal, and hydraulic flow characteristics in the system. The iterative solution of this method is higher than that of the traditional Newton–Raphson iterative method, which can improve the operation economy



**Citation:** Wang, Q.; Cheng, S.; Ma, S.; Chen, Z. Multi-Time Interval Dynamic Optimization Model of New Energy Output Based on Multi-Energy Storage Coordination. *Electronics* **2023**, *12*, 3056. <https://doi.org/10.3390/electronics12143056>

Academic Editor: Yushuai Li

Received: 21 June 2023

Revised: 6 July 2023

Accepted: 10 July 2023

Published: 12 July 2023



**Copyright:** © 2023 by the authors. Licensee MDPI, Basel, Switzerland. This article is an open access article distributed under the terms and conditions of the Creative Commons Attribution (CC BY) license (<https://creativecommons.org/licenses/by/4.0/>).

of the multi-energy system. At present, most of the research on the energy balance of multi-energy power grids still stays at the day-ahead scheduling level. At the intra-day level, there are few studies on real-time energy balance considering new energy fluctuations.

Aiming at the control problem of the new energy stable operation domain, a multi-period planning model of a multi-energy microgrid is proposed in Reference [10], and the enhanced bilinear Benders decomposition method is used to solve the model, which can effectively deal with the influence of multi-type uncertainties on the system. Reference [11] established a multi-energy coordinated scheduling model based on the hybrid stochastic interval method so that the system can still maintain efficient operation under multiple uncertainties. Reference [12] studied a stability region analysis method of the droop coefficient of a new energy inverter, which can obtain a more accurate coordinated stability region of the droop coefficient and provide support for the optimal scheduling of the system. Reference [13] proposed a two-stage robust operation method for multi-energy systems considering uncertainties, which uses multi-energy complementary coordination to compensate for multi-dimensional uncertainties and maintain the energy balance of the system. Reference [14] proposed a robust flexible scheduling method for multi-energy systems that can improve the flexibility of demand-side response. The above research results provide some solutions for the new energy output control of multi-energy systems in uncertain scenarios. However, in the study of real-time control of new energy output, how to achieve rapid suppression of new energy fluctuations while taking into account the economy is subject to improvement.

Therefore, this paper proposes a multi-period interval dynamic optimization model of new energy output based on multi-energy storage coordination. The specific innovative research results are as follows:

- (1) To realize the dynamic optimization of new energy output, the optimal solution of new energy output is discretized to form a continuous function in time.
- (2) A dynamic optimization strategy is designed, which regards the multi-energy energy storage device and the new energy unit as a whole. By controlling the state of charge of the energy storage device, the output fluctuation of the new energy is suppressed.
- (3) Considering the adjustment cost of multiple types of regulating equipment connected to multi-energy power systems, the objective function of new energy output optimization of multi-energy power systems is established, and the model is solved based on distributed graph theory.

## 2. Multi-Energy Storage Model

### 2.1. Electrothermal Energy Storage Model

The energy conversion process in the high-voltage electric heating and storage system can be described as three stages: the electric heating stage, heat storage stage, and heat release stage [15].

For the electric heating stage, the heat absorbed by the heat storage system is provided by the electrothermal resistance wire, assuming that the conversion efficiency of electricity to heat is  $\eta_{ht}$ , then:

$$P_{inQ} = \eta_{ht} P_{hin} \quad (1)$$

where  $P_{hin}$  is the input power of heat storage,  $P_{inQ}$  is the absorption power of heat storage.

For the heat storage stage and the heat release stage, the energy state of the system can be expressed by the following equation:

$$\Delta E_{pQ} = (P_{inQ} - P_{outQ} - P_{lost}) \Delta t \quad (2)$$

where  $\Delta E_{pQ}$  is the energy change in the heat storage system,  $P_{inQ}$  is the heat absorbed by the heat storage system,  $P_{outQ}$  is the heat supplied by the heat storage system, and  $P_{lost}$  is the power lost by the heat storage system in unit time.

## 2.2. Battery Characteristic Model

The storage and release characteristics  $W_e(t)$  of electrical energy during battery charging and discharging [16] can be described as:

$$W_e(t) = \int_{t-\Delta t}^t S_{be}^2 [i_{eec}(t) + i_{lec}(t)]^2 R_B dt + k_{iust}(t) \int_{t-\Delta t}^t S_{be} [i_{eec}(t) + i_{lec}(t)] U_F(t) dt \quad (3)$$

where  $k_{iust}(t)$  is the battery charge and discharge state function, the value is  $-1$  or  $+1$ , which represents the charging and discharging states, respectively;  $R_B$  is the equivalent resistance between the positive and negative poles of the battery;  $U_F$  is the potential difference between the positive and negative electrodes of the battery.

## 2.3. Electro-Hydrogen Energy Storage Characteristic Model

The electric hydrogen energy storage system mainly includes three components: electrolysis of water to hydrogen, hydrogen storage, and hydrogen fuel cell power generation [17,18].

Electro-hydrogen energy conversion characteristics can be described as:

$$W_{TH}(t) = \frac{\eta_{TH}}{Q_{H_2}} \int_{t-\Delta t}^t P_{TH}(t) dt \quad (4)$$

where  $W_{TH}$  is the energy contained in the hydrogen produced by the electrolysis of the water hydrogen production device in  $\Delta t$  time scale;  $P$  is the power consumption of the water electrolysis hydrogen production device in  $\Delta t$  time scale;  $\eta_{TH}$  and  $Q_{H_2}$  are the electro-hydrogen energy conversion efficiency of the electrolysis water hydrogen production device and the calorific value per unit volume of hydrogen, i.e., the chemical energy contained in the unit volume of hydrogen.

The hydrogen-electric energy conversion characteristics of hydrogen fuel cells can be expressed as:

$$W_{Hout}(t) = Q_{H_2} \eta_{ch} W_{Hin}(t) \quad (5)$$

$$W_{Hin}(t) = \int_{t-\Delta t}^t V_{Hin}(t) dt \quad (6)$$

where  $W_{Hout}$  is the electrical energy emitted by the hydrogen fuel cell in  $\Delta t$  time scale;  $W_{Hin}(t)$  is the hydrogen fuel cell consuming hydrogen energy at  $\Delta t$  time scale;  $V_{Hin}$  is the hydrogen consumption rate of the hydrogen fuel cell at  $\Delta t$  time scale ( $m^3/h$ );  $\eta_{ch}$  and  $Q_{H_2}$  are the hydrogen-electric energy conversion efficiency of the hydrogen fuel cell and the calorific value per unit volume of hydrogen, respectively.

The amount of hydrogen stored in the hydrogen storage tank and the energy characteristics contained in it can be expressed as:

$$W_{HST}(t) = W_{HST}(t - \Delta t) - \gamma_{Hin} Q_{H_2} \int_{t-\Delta t}^t V_{Hin}(t) dt \quad (7)$$

where  $W_{HST}(t)$  is the energy contained in the hydrogen storage device at time  $t$ ;  $W_{HST}(t - \Delta t)$  is the energy contained in the hydrogen storage device before  $\Delta t$ ;  $V_{Hin}(t)$  is the amount of hydrogen injected into the compressor, which may be positive or negative;  $\gamma_{Hin}$  and  $Q_{H_2}$  are the hydrogen compression injection efficiency and calorific value per unit volume of hydrogen, respectively.

## 3. Dynamic Optimization Strategy of New Energy Output Based on Multi-Energy Storage Control

Based on a thorough analysis of the operational characteristics of multi-energy storage devices, this section takes advantage of the fast response and strong regulation ability of energy storage devices, and considers the multi-energy storage devices and new energy

units as a whole, designing a dynamic optimization strategy. By controlling the state of charge of the energy storage device, the fluctuation of new energy output can be suppressed.

### 3.1. Discretization Optimization of New Energy Output

To realize the dynamic optimization of new energy output, the optimization solution of new energy output needs to be regarded as a continuous function in time [19]:

$$\min_{p(t)} z = \phi(g) \quad (8)$$

$$st. \begin{cases} \dot{m} = F_{EPS}(m, p, d), m(0) = m_0 \\ g = F_{EOU}(m, p) \\ p_i \leq p(t) \leq p_x \end{cases}$$

where  $z$  is the objective of minimizing fluctuations in the new energy output of a multi-energy power system;  $F_{EPS}(\cdot)$  is the equation of state for a multi-energy power system;  $g \in R^{n_g}$  is the output power of each wind and photovoltaic station in the multi-energy power system;  $F_{EOU}(\cdot)$  is the output equation of a new energy generation system for a multi-energy power system;  $m \in R^{n_m}$  is the state variables of voltage magnitude, phase angle, line active power and line reactive power in a multi-energy power system;  $m_0$  is the initial state of the multi-energy power system at time  $t = 0$ ;  $d \in R^{n_d}$  is an uncertain disturbance causing fluctuations in wind and PV output in a multi-energy power system;  $p(t) \in R^{n_p}$  is the amount of input and output power control for all adjustable devices in a multi-energy power system including each multi-energy storage system;  $p_i$  and  $p_x$  are the lower and upper limits of power regulation for each adjustable device, respectively;  $\phi(\cdot)$  is the objective function for optimizing the power output of new energy sources in a multi-energy power system, which can be expressed by the power output characteristics of the wind and photovoltaic power systems operating in the system.

$$\phi(g) = \max \left| P_{MPE} - \left( \sum_{i=1}^{x_{WP}} g_i + \sum_{j=1}^{x_{PV}} g_j \right) \right| \quad (9)$$

where  $P_{MPE}$  is the total new energy output forecast for the multi-energy power system;  $g_i$  is the  $i$ -th equivalent wind turbine or wind farm output in a multi-energy power system;  $x_{WP}$  is the number of equivalent wind turbines or wind farms in a multi-energy power system;  $g_j$  is in a multi-energy power system  $j$ -th equivalent PV unit or PV plant output;  $x_{PV}$  is the number of equivalent PV units or PV plants in a multi-energy power system.

The above dynamic process of optimizing the new energy output is discretized into a non-linear programming problem in each sub-time interval and can be described as:

$$\min_{p_i, \dots, p_{N_{EIC}}} z = \phi[g(N_{EIC})] \quad (10)$$

$$st. \begin{cases} m(i+1) = F_{DJK}[m(i), p(i), d(i)], m(0) = m_0 \\ g(i) = P_{OUE}[m(i), p(i)] \\ p_i \leq p(i) \leq p_x \\ \forall i = 1, \dots, N_{EIC} \end{cases}$$

where  $N_{EIC}$  is the number of sub-time intervals of the multi-energy power system within a dispatch time interval period  $[0, T_{EIC}]$ ;  $F_{DJK}$  and  $p_{OUE}$  are the non-linear equation of state of the multi-energy power system and the new energy power output equation, respectively after discretization according to the dispatch time interval.

### 3.2. Dynamic Optimization Strategy for New Energy Output

Based on the optimal discretization of new energy output, this paper proposes an optimal control method of new energy output considering the state of multi-energy storage sources, which can quickly respond to the uncertain disturbance with time-varying characteristics in the scheduling time interval.

### 3.2.1. New Energy Unit Output Matrix Considering Multi-Energy Storage Control and Uncertainty Disturbance

In the dynamic optimization process, the scheduling time interval needs to be divided into several time subintervals. In each time subinterval, the proportion of new energy output in the system is set unchanged. When a time subinterval ends, the given value of the new energy output of the next subinterval is corrected according to the real-time output of each unit at the end time. When the whole scheduling interval ends, the proportion of new energy output is reset according to the set value of new energy output in the next scheduling interval, and so on.

Divide the scheduling time interval  $[0, T_{EIC}]$  into  $N_{EIC}$  sub-time intervals:

$$[0, t_1), [t_1, t_2), \dots, [t_{i-1}, t_i), \dots, [t_{EIC-1}, t_{EIC}) \tag{11}$$

where  $i \in 1, 2, \dots, N_{EIC}$  is the  $i$ -th sub-time interval. Then, the optimization objective of the new energy output in the multi-energy power system on the  $i$ -th sub-time interval  $[t_{i-1}, t_i)$  can be expressed as:

$$F_{EOT}(i) = O_{EOT}g(i) \tag{12}$$

where  $F_{EOT}(i)$  is the set value of new energy output in the  $i$ -th sub-time interval  $[t_{i-1}, t_i)$  of the multi-energy power system within the scheduling time interval  $[0, T_{EIC}]$  determined by the previous day's dispatch;  $g(i)$  is the output of each equivalent new energy unit or new energy station in the multi-energy power system in the  $i$ -th sub-time interval  $[t_{i-1}, t_i)$ ;  $O_{EOT}$  is the given combination conversion matrix, which describes the proportion of the output of each equivalent new energy unit or new energy station in the multi-energy power system within the scheduling time interval  $[0, T_{EIC}]$  determined by the previous day's dispatch. The share of the capacity of the new energy unit or new energy station in the multi-energy power system in the time interval  $[0, T_{EIC}]$  determined at the time of dispatch.

To solve the optimal combination matrix that satisfies the general situation of new energy output uncertainty in a multi-energy power system  $O_{EOT}$ , it is necessary to determine the actual value of new energy output under actual operating conditions. Here, this paper considers the influence of disturbance deviation on system operation, and defines the actual output deviation function of new energy  $K_{DUEF}$  as follows:

$$K_{DUEF} = Z(p, \mathbf{d}) - Z_{IET}(\mathbf{d}) \tag{13}$$

where  $Z_{IET}$  is the minimum value of the actual fluctuation of the new energy output of the multi-energy power system.

Under the premise of a given uncertainty disturbance  $\mathbf{d}$  of the actual output of new energy, the objective of minimizing the fluctuation of new energy output  $Z(p, \mathbf{d})$  can be transformed into a second-order function of the actual control of multi-energy storage devices  $p_{IET}$  in the system:

$$Z(p, \mathbf{d}) = Z_{IET}(\mathbf{d}) + \frac{\partial Z(p - p_{IET})}{\partial p} + \frac{1}{2}(p - p_{IET}) \frac{\partial^2 Z(p - p_{IET})}{\partial p^2} \tag{14}$$

Since the proportion of new energy output is constant in the time subinterval, the objective function satisfies:

$$\frac{\partial Z(p - p_{IET})}{\partial p} = 0 \tag{15}$$

Then, from the above equation and the actual new energy output deviation function  $K_{DUEF}$  can be obtained as follows:

$$K_{DUEF} = \frac{1}{2}(p - p_{IET}) \frac{\partial^2 Z(p - p_{IET})}{\partial p^2} \tag{16}$$

At this point, the new energy output of the multi-energy power system, as determined by the previous day's dispatch, is expressed as:

$$g = F_{OUE}p + F_{DJK}d \tag{17}$$

After considering the influence of disturbance bias in the system, the error in the output of new energy in the system can be expressed as:

$$\Delta p = -(O_{EOT}F_{OUE})^{-1}O_{EOT}F_{DJK}\Delta d \tag{18}$$

From this, the control deviation of the multi-energy storage system in actual operation can be given as:

$$\Delta p_{IET} = -\frac{\frac{\partial^2 Z(p-p_{IET})}{\partial p \partial d}}{\frac{\partial^2 Z(p-p_{IET})}{\partial p^2}} \Delta d \tag{19}$$

Thus, the deviation of the new energy output of the multi-energy power system from the optimized output value set by the previous day's dispatch during the actual grid operation can be found  $K_{DUEF}$ , as:

$$K_{DUEF} = \frac{1}{2} \left\| S(O_{EOT}F_{OUE})^{-1}O_{EOT}\alpha \right\|_2^2 \tag{20}$$

where  $S^T S = \frac{\partial^2 Z(p-p_{IET})}{\partial p^2}$ ,  $\alpha = -\left(F_{OUE} \frac{\partial^2 Z(p-p_{IET})}{\partial p^2}\right)^{-1} \frac{\partial^2 Z(p-p_{IET})}{\partial p^2}$ .

According to the above equation, considering the actual operating conditions of the multi-energy power system in each time interval, the matrix  $O_{EOT}$  of the power output of each equivalent new energy unit or new energy station in the system can be given as:

$$O_{EOT}^T = \frac{\sqrt{\frac{\partial^2 Z(p-p_{IET})}{\partial p^2}}}{(\alpha\alpha^T)F_{OUE} \left(F_{OUE}^T(\alpha\alpha^T)^{-1}F_{OUE}\right)} \tag{21}$$

### 3.2.2. Dynamic Optimization of New Energy Output Combination Matrix

To enable various equipment in a multi-energy system to continuously change their output status according to the regulatory requirements of the power grid during actual operation, it is necessary to continuously adjust the proportion of new energy units in the system. Therefore, the output combination matrix of new energy is constantly revised with the increase of subintervals.

The proportion of new energy power output in the  $i$ -th time subinterval during  $[0, T_{EIC}]$  is determined by the actual new energy output in all operated subintervals before, namely:

$$F_{EOT}(i) = F_{EOT}(i-1) - O'_{EOT} \begin{bmatrix} g(0) \\ g(1) \\ \vdots \\ g(i-1) \end{bmatrix} \tag{22}$$

where  $g(i-1)$  is the output of each equivalent new energy unit or new energy station in the multi-energy power system in the  $i$ -th sub-time interval  $[t_{i-2}, t_{i-1}]$ ;  $O'_{EOT}$  is a modified

combination matrix based on the new energy output of the previous  $i - 1$  sub-time interval, given by the following equation:

$$O'_{EOT} = \begin{bmatrix} [O'_{EOT1}O_{EOT}] & 0 & \cdots & 0 \\ 0 & [O'_{EOT2}O_{EOT}] & \cdots & 0 \\ \vdots & \vdots & \ddots & \vdots \\ 0 & 0 & \cdots & [O'_{EOTi}O_{EOT}] \end{bmatrix} \quad (23)$$

where  $O'_{EOTi}$  is the proportional adjustment matrix for the combination of new energy power output set for each time subinterval.

After taking into account the correction of the new energy output mix ratio by the operating state of the  $N_{EIC}$  time subintervals during  $[0, T_{EIC}]$ , by the combination conversion matrix  $O_{EOT}$  determined by the previous day's scheduling and the new energy output mix ratio adjustment matrix  $O'_{EOT}$  the new energy output optimization target for the next scheduling time interval is initialized:

$$F'_{EOT,N+1} = F_{EOT,N+1} + O_{EOT,N+1} \begin{bmatrix} O_{EOT}g(1) + O'_{EOT1}G_{OUE}[g(0)] \\ O_{EOT}g(2) + O'_{EOT2}G_{OUE}[g(0), g(1)] \\ \vdots \\ O_{EOT}g(N_{EIC}) \\ + O'_{EOTN_{EIC}}G_{OUE}[g(0), g(1), \dots, g(N_{EIC})] \end{bmatrix} \quad (24)$$

where  $F_{EOT,N+1}$  and  $F'_{EOT,N+1}$  are the day-ahead setting and the corrected setting of the new energy power output at the beginning of the next day-ahead dispatch time interval after the end of  $[0, T_{EIC}]$ , respectively;  $O_{EOT,N+1}$  is the combination matrix of new energy power output at the beginning of the next day-ahead dispatch time interval as determined by day-ahead dispatch;  $G_{OUE}(\cdot)$  is the cumulative correction function for fluctuations in new energy output in the previous day's dispatch interval.

#### 4. Optimization Model for New Energy Output from Multi-Energy Grids

##### 4.1. Objective Function

Considering the multi-energy forms connected to the multi-energy power system, electricity to heat and electricity to hydrogen are the mainstay, and the regulation resources participating in the coordinated optimization of new energy output include thermal power, hydropower, wind power, photovoltaic and electric heating energy storage, electricity hydrogen energy storage and battery energy storage. The objective function of new energy output optimization of multi-energy power system comprehensively considering the regulation cost of each regulating resource is:

$$\min f_{COST}[z(p, \mathbf{d})] = f_{COST} \left( \sum_{i=1}^n CST_{i,T} \right) \quad (25)$$

where  $f_{COST}$  is the regulation cost function of a multi-energy power system for a given new energy output fluctuation optimization objective;  $CST_{i,T}$  is the cost function of each regulating resource participating in the regulation of the new energy output of the grid during the time interval of each day of dispatch of the multi-energy power system, which is thermal power regulation cost function, hydropower regulation cost function, heat storage regulation cost function, electricity storage regulation cost function, hydrogen storage regulation cost function and load regulation cost function.

## 4.2. Constraints

### 4.2.1. Multi-Energy Power System New Energy Output Regulation Range Trade-Off Constraint

Multi-energy power system new energy output regulation range trade-off constraint is shown as:

$$P_{DUOP,T}^{\min} \leq P_{DUOP,T} \leq P_{DUOP,T}^{\max} \quad (26)$$

where  $P_{DUOP,T}$  is the total new energy output expected from the multi-energy power system during the dispatch time interval  $T$ ;  $P_{DUOP,T}^{\max}$  and  $P_{DUOP,T}^{\min}$  are the expected upper and lower limits of fluctuations in the total new energy output of the multi-energy power system during the dispatch time interval  $T$ . The significance of these two parameters is to determine a reasonable expectation of a fluctuating range of new energy output, too large an expectation can cause lead to a lower level of system power balance, while too small an expectation can cause higher regulation costs.

### 4.2.2. Constraints on the Regulation Characteristics of Thermal and Hydropower Units

For thermal and hydropower units, the regulation performance and scope of their participation in the optimization of the new energy output of a multi-energy power system is mainly governed by two indicators: the adjustable power size and the adjustable power variation rate:

$$\begin{cases} \Delta P_{H\&W,T}^{\min} \leq \Delta P_{H\&W,T} \leq \Delta P_{H\&W,T}^{\max} \\ K_{H\&W,T}^{\min} \leq K_{H\&W,T} \leq K_{H\&W,T}^{\max} \end{cases} \quad (27)$$

where  $\Delta P_{H\&W,T}$  is the adjustable power of thermal or hydropower units of the multi-energy power system during the dispatch time interval  $T$ ;  $\Delta P_{H\&W,T}^{\max}$  and  $\Delta P_{H\&W,T}^{\min}$  are the upper and lower limits of the adjustable power of a multi-energy power system for thermal or hydropower, respectively, during the dispatch time interval  $T$ ;  $K_{H\&W,T}$  schedules the rate of change in the adjustable power of thermal or hydro units of a multi-energy power system during the time interval  $T$ ;  $K_{H\&W,T}^{\max}$  and  $K_{H\&W,T}^{\min}$  are the upper and lower limits for the rate of change in the adjustable power of a multi-energy power system, thermal or hydro, respectively, during the dispatch time interval  $T$ .

In general, the regulable power of thermal or hydropower units is reserved in advance of the daily or weekly dispatch cycle, while the regulation rate is related to the technical performance of the unit and its power system. A larger reserved regulation power and a better regulation rate also correspond to a larger regulation cost. Therefore, in multi-energy power systems with a large proportion of new energy sources, the potential for multi-energy interaction and storage should be exploited as much as possible, to reduce the reserved regulation power of thermal or hydropower units and thus reduce the cost of optimizing the new energy generation output of the multi-energy power system.

### 4.2.3. Multi-Energy Storage Regulation Characteristics Constraints

For thermal, electrical, and hydrogen storage systems, the regulation performance and range of the systems involved in optimizing the new energy output of a multi-energy power system is governed by the State of Charge (SOC) adjustable power and the rate of change in adjustable power:

$$\begin{cases} SOC_{MES,T}^{\min} \leq SOC_{MES,T} \leq SOC_{MES,T}^{\max} \\ |\Delta P_{MES,T}^{\min}| \leq |\Delta P_{MES,T}| \leq |\Delta P_{MES,T}^{\max}| \\ |K_{MES,T}^{\min}| \leq |K_{MES,T}| \leq |K_{MES,T}^{\max}| \end{cases} \quad (28)$$

where  $SOC_{MES,T}$  is the multi-energy storage load state in the dispatch time interval  $T$ ;  $SOC_{MES,T}^{\max}$  and  $SOC_{MES,T}^{\min}$  are the upper and lower limits of the multi-energy storage load state in the dispatch time interval;  $\Delta P_{MES,T}$  is the adjustable power of multi-energy storage charging and discharging energy in the dispatching time interval  $T$ ;  $\Delta P_{MES,T}^{\max}$  and  $\Delta P_{MES,T}^{\min}$  are the upper and lower limits of the adjustable power of multi-energy charging and

discharging energy in the dispatching time range;  $K_{MES,T}$  dispatch time interval  $T$  multi-energy storage charging and discharging power change rate;  $K_{MES,T}^{\max}$  and  $K_{MES,T}^{\min}$  are the upper and lower limits of the adjustable power change rate of multi-energy storage charging and discharging energy in the dispatching time interval  $T$ .

#### 4.2.4. Multi-Energy Regulation Balance Constraints

Regardless of the electricity, heat, hydrogen, and gas systems, when it is necessary to ensure participation in the optimization of the new energy output of a multi-energy power system within a given time scale, its regulation performance and scope are mainly constrained by the two indicators of State of Charge (SOC) adjustable power size and adjustable power change rate:

$$\sum_{zm \in MESi} W_{MES,T} + \sum_{zr \in h\&w} W_{H\&W,T} + \sum_{zr \in DRMi} W_{DRM,T} = \Delta W_{\Sigma} \tag{29}$$

where  $W_{MES,T}$  is the regulation energy of multi-energy storage in the dispatching time interval  $T$ ;  $W_{H\&W,T}$  is the regulation energy of thermal power and hydropower units in the dispatching time interval  $T$ ;  $W_{DRM,T}$  is the response load regulation energy of the demand side in the dispatching time interval  $T$ ;  $\Delta W_{\Sigma}$  is the total energy demand of the multi-energy power system in the dispatching time interval  $T$  to optimize the output of new energy.

#### 4.2.5. Multi-Energy Power System Network Constraints

$$\begin{cases} P_{supply,i,T} = P_{con,i,T} + V_i \sum_{j \in i} V_j (G_{ij} \cos \theta_{ij} + B_{ij} \sin \theta_{ij}) \\ Q_{supply,i,T} = Q_{con,i,T} + V_i \sum_{j \in i} V_j (G_{ij} \sin \theta_{ij} - B_{ij} \cos \theta_{ij}) \end{cases} \tag{30}$$

where  $P_{supply,i,T}$  and  $Q_{supply,i,T}$  provides active power and reactive power to multi-energy power system nodes  $i$  in the scheduling time intervals  $T$  of thermal power, hydropower, wind power, photovoltaic, and battery energy storage, respectively;  $P_{con,i,T}$  and  $Q_{con,i,T}$  represents the active power and reactive power consumed by the nodes  $i$  in the multi-energy power system in the scheduling time interval  $T$ , respectively, for electric heating energy storage, electric hydrogen energy storage, and electric load;  $G$ ,  $B$  and  $\theta$  are conductance, susceptance and voltage phase angle difference between adjacent nodes of multi-energy power system, respectively.

$$\begin{cases} U_{i,T}^{\min} \leq U_{i,T} \leq U_{i,T}^{\max} \\ (I_{ij,T}^{\min})^2 \leq I_{ij,T}^2 \leq (I_{ij,T}^{\max})^2 \end{cases} \tag{31}$$

where  $U_{i,T}^{\max}$  and  $U_{i,T}^{\min}$  are the upper and lower limits of the node voltage amplitude in the scheduling time interval  $T$ ;  $I_{ij,T}^{\max}$  and  $I_{ij,T}^{\min}$  are the upper and lower limits of branch current in the scheduling time interval  $T$ .

#### 4.3. Solving Algorithm

Based on the proposed optimization strategy for new energy output, this paper solves the model using a directed graph topology distributed algorithm [20]. The distributed power supply in a multi-energy system has the characteristics of plug-and-play. Therefore, the distributed algorithm using directed graph topology can adapt to the changing structure of a multi-energy power grid and quickly solve the problem of changing topology. The multi-energy storage devices involved in the multi-energy system and the distribution characteristics and energy interaction relationship of multi-energy generation units can be represented as a directed graph composed of nodes and connection relationships:

$$G_{COST} = \{V_{COST}, E_{COST}, A_{COST}\} \tag{32}$$

where  $V_{COST}$  is the set of nodes with the flexibility to regulate resources in the multi-energy power system;  $E_{COST}$  is the set of connection relationships between flexible resource nodes with energy interaction in multi-energy power systems;  $A_{COST}$  is the energy interaction intensity matrix between flexible resource nodes in multi-energy power systems.

In the directed graph, the objective function for optimizing the new energy output of the multi-energy power system can be expressed as a function of the three-dimensional variable  $g_{COSTi}$  for the input and output power of electricity, heat, and hydrogen energy:

$$\min f_{COST}[Z(p, \mathbf{d})] = F_{COST} \left( \sum_{i=1}^N g_{COSTi,T} \right) \tag{33}$$

where  $N$  is the number of nodes in the multi-energy power system with flexible regulation resources and  $F_{COST}$  is the network-wide regulation cost function of the multi-energy power system.

Before the start of the scheduling time interval, the basic operating status of the nodes in the multi-energy power system network can be obtained as:

$$U_{ij,T} = [U_{EL,ij,T}, U_{TH,ij,T}, U_{H2ij,T}]^T \tag{34}$$

The objective function for optimizing the new energy output of a multi-energy power system according to the above equation can then be further rewritten in the following form:

$$\begin{cases} \min F_{COST} \left( \sum_{i=1}^N \sum_{j=1}^N (g_{COSTii,T} + \omega_{COSTij,T} g_{COSTij,T}) \right) \\ \text{s.t. } \sum_{i=1}^N g_{COSTi} = \sum_{i=1}^N \sum_{j=1}^N U_{ij,T}, g_{COSTi,T} \in \gamma_{COSTij} \end{cases} \tag{35}$$

According to the objective function shown above, the adjustment demand capacity of each node during the scheduling time interval  $\Delta U_{ij,T}$  can be obtained by solving it. Therefore, the optimization and regulation goal of new energy output is:

$$\begin{aligned} & [\Delta U_{EL,ij,T}, \Delta U_{TH,ij,T}, \Delta U_{H2ij,T}] \nabla F_{COSTij,T} \\ & = 2\varphi_{EL,ij,T} \|\Delta U_{EL,ij,T}\|^2 + 2\varphi_{TH,ij,T} \|\Delta U_{TH,ij,T}\|^2 + 2\varphi_{H2ij,T} \|\Delta U_{H2ij,T}\|^2 \\ & \geq \Phi_{ij,T} \|\Delta U_{EL,ij,T}, \Delta U_{TH,ij,T}, \Delta U_{H2ij,T}\|^2 \end{aligned} \tag{36}$$

where  $\nabla$  is the scatter of the  $F_{COSTij,T}$  function within the scheduling time interval; and  $\Phi_{ij,T}$  is given by:

$$\Phi_{ij,T} = \min \{ \varphi_{EL,ij,T}, \varphi_{TH,ij,T}, \varphi_{H2ij,T} \} \tag{37}$$

where  $\varphi_{EL,ij,T}$ ,  $\varphi_{TH,ij,T}$  and  $\varphi_{H2ij,T}$  are the regulation cost coefficients of the flexibility resource nodes when they participate in the optimization of the new energy output of the multi-energy power system with the corresponding regulation energy of  $\Delta U_{EL,ij,T}$ ,  $\Delta U_{TH,ij,T}$  and  $\Delta U_{H2ij,T}$  for electricity, heat, and hydrogen, respectively. In this study, all flexible resources are assumed to have positive electricity, heat, and hydrogen energy regulation costs greater than zero when participating in the optimization of new energy output from a multi-energy power system as  $\Phi_{ij,T} > 0$ .

### 5. Example Analysis

According to the actual structure and operation data of a power grid, this paper establishes a simulation system. A multi-energy power system topology including new energy power supply represented by wind and photovoltaic power generation and other multi-

energy exchange and storage equipment is constructed, as shown in Figure 1. The capacity configuration of each power supply and energy storage device is shown in Tables 1 and 2.

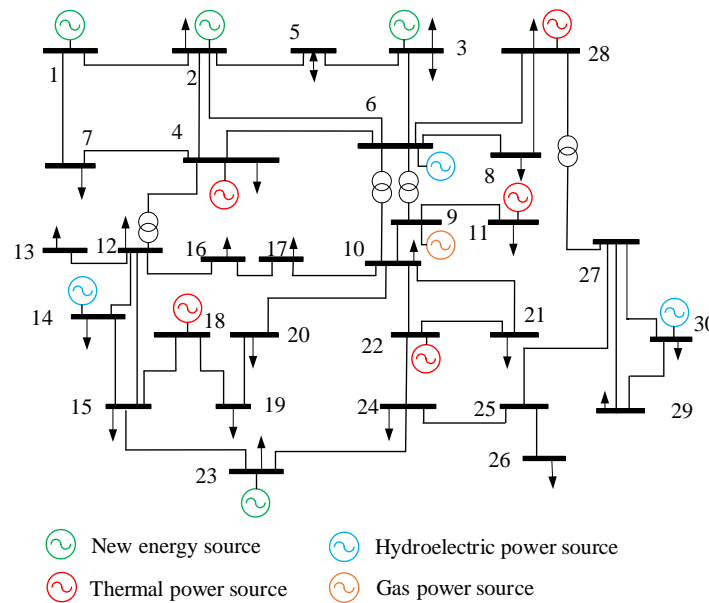


Figure 1. Topology of new energy power system.

Table 1. Capacity parameter of power source.

Node Number	Power Source Type	Capacity (MW)
1, 3, 23	Wind power	11,000
2	Photovoltaic power	4800
4, 11, 18, 22, 28	Thermal power	36,500
14, 6, 30	Hydroelectric power	3000
9	Gas power	1500

Table 2. Capacity parameter of multi-energy storage equipment.

Node Number	Power Source Type	Capacity (MWh)
8, 9	Electric heating and heat storage equipment	11,000
5	Electric hydrogen production, hydrogen storage equipment, and hydrogen cell	4800
7, 24	Chemical battery	1500

To verify the effectiveness of the proposed dynamic optimization method for multi-energy systems that considers multi-source energy storage coordination and disturbance of new energy output, the following simulation scenarios are set up to validate the proposed method, as shown in Table 3.

Table 3. Simulation scenario setting.

Simulation Scenario	Whether the Energy Storage Device Is Involved in Regulation	New Energy Output Uncertainty	Algorithm
S1	NO	5%	Proposed algorithm
S2	YES	5%	Proposed algorithm
S3	YES	20%	Proposed algorithm
S4	YES	20%	Multi-objective differential algorithm

### 5.1. The Influence of Energy Storage Configuration on the Optimization Results

To study the necessity of multi-energy storage devices in optimizing new energy output, this article sets up S1 and S2 for comparison. Optimize and solve the output of multi-energy system units with a 5% uncertainty in new energy output.

According to the actual operation data of the new energy power grid. Provide the wind power output, photovoltaic output, and load demand curves of the multi-energy system as shown in Figure 2. It can be seen from Figure 2 that the photovoltaic output period is from 7:00 to 18:00, the wind farm outputs electric energy throughout the day, and the output is more at night. Comparing the new energy output with the load curve, it can be seen that in the two periods of 6:00–12:00 and 18:00–22:00, the trend of the new energy output and the load demand curve is inconsistent. Therefore, in the optimization process, energy storage devices are needed to supplement the new energy output in these two periods.

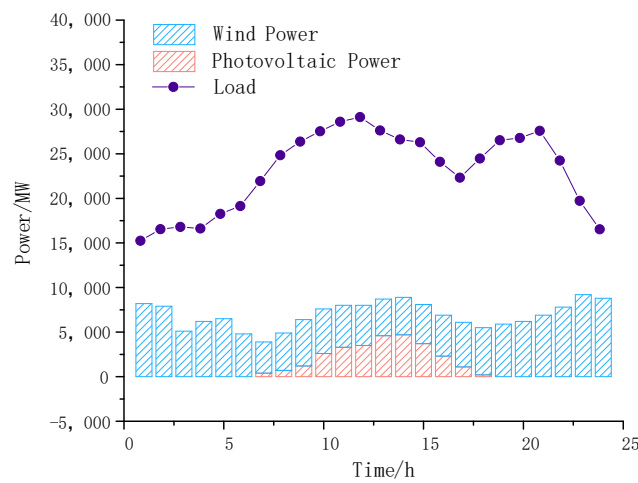


Figure 2. Multi-energy power system typical new energy power output and load curve.

S1:

Regarding the new energy output and load curve of the multi-energy system shown in Figure 2, in the scenario where energy storage is not involved in regulation when the new energy generation output of the system fluctuates, the main units responsible for peak-shaving in the system are thermal power, hydropower, and gas units. At this point, to adapt to the fluctuation of new energy output, the variation characteristics of the hydroelectric output, thermal power output, and gas power generation output curves of the multi-energy system are shown in Figure 3.

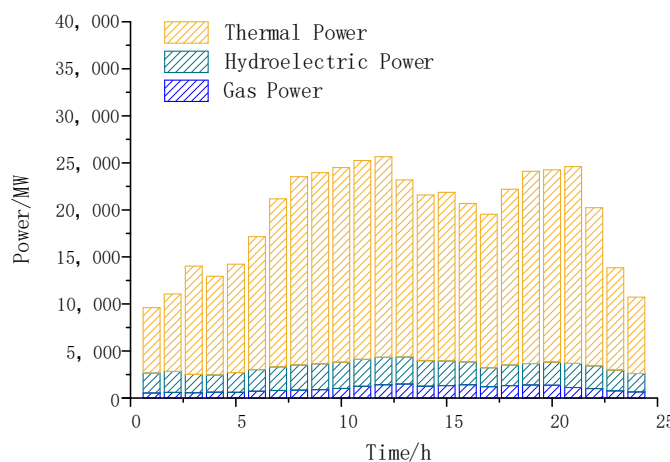


Figure 3. Traditional power unit output under S1.

From Figure 3, it can be seen that to make the power grid can still meet the balance of supply and demand power under the premise of fluctuation of new energy power generation, it is necessary to start up a large thermal power and gas turbine. The greater the start-up mode of these two types of units, the higher the carbon emissions of multi-energy power systems. In addition, some thermal power, hydropower, and gas units in the running time of the production of electricity than the load demand, which caused some unnecessary waste.

S2:

When there are fluctuations in the output of new energy, consider the participation of multiple energy storage systems such as electric heat storage, chemical batteries, electric hydrogen storage, and hydrogen fuel cells in regulation. At this point, the optimization results of new energy output are shown in Figure 4, and the output curve of traditional generator sets is shown in Figure 5.

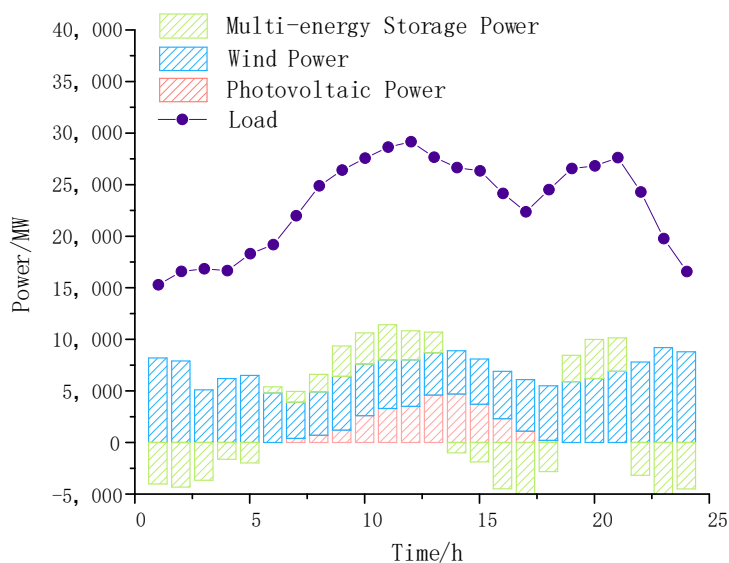


Figure 4. New energy power output optimization under S2.

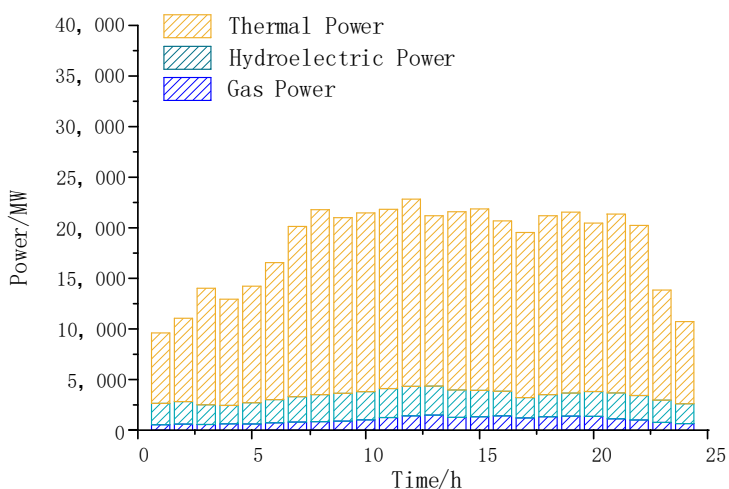


Figure 5. Traditional power unit output under S2.

As shown in Figure 4, in the scenario where multi-energy storage is involved in regulation, the charging and discharging power of the energy storage device can suppress the fluctuation of new energy output, making its output characteristics more in line with the load demand power curve. From Figure 5, it can be seen that the output of traditional generator sets has significantly decreased compared to S1, and the peak-shaving pressure

has significantly decreased. At this time, in addition to traditional power regulation resources, the conversion and storage coordination of multiple energy sources in the system effectively reduces the dependence of power system peak-shaving on thermal power units, gas units, and hydropower units.

On the other hand, after combining the three forms of energy storage, each participates in the optimization and regulation of the multi-energy power system, which can give full play to the regulation potential of various energy storage devices and achieve better complementarity with new energy output. When the output of new energy is greater than the load, it absorbs energy in time, reduces the abandonment of wind and light in the system, participates in peak-shaving when the output of new energy is low and the load is at its peak and reduces the burden on the power grid. This verifies the necessity of multi-energy storage devices participating in the regulation of new energy output optimization.

The output cost of each peak-shaving unit in the system is shown in Figure 6.

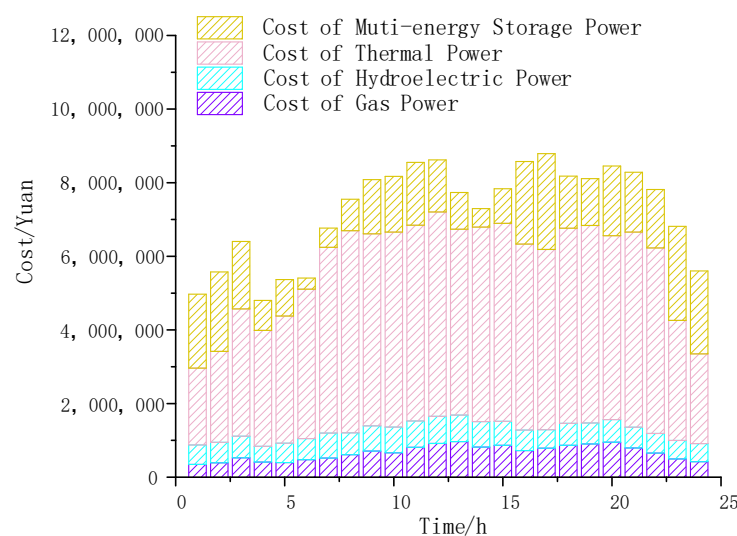


**Figure 6.** Multi-energy power system peak-shaving cost under S2.

### 5.2. The Influence of New Energy Output Uncertainty on the Optimization Results

To study the impact of uncertainty in new energy output on the optimization results, this paper sets S3 and compares it with S2 under the premise of only increasing uncertainty in new energy output under the same other conditions.

S3:

If a 20% random change in the uncertainty of new energy output is made, the system load demand is the same as shown in Figure 2. When the uncertainty of new energy output is 20%, the optimization algorithm proposed in this article is used. The output optimization results of new energy units are shown in Figure 7, while the output results of traditional power generation units are shown in Figure 8.

From the simulation results in Figure 7, it can be seen that in the case of a 15% increase in uncertainty of new energy output, the effect of energy storage devices on optimizing new energy output fluctuations is slightly weaker than in S2. During the peak period of new energy output, the charging energy of the energy storage device is slightly less than that of S2, and the regulating output of the energy storage device is also slightly reduced during the peak period of low load demand of new energy output. However, they can still make some extent suppress new energy fluctuations.

From the simulation results in Figure 8, it can be seen that in response to the impact of increased uncertainty in new energy output, the reserve capacity in the multi-energy system is increased compared to S1 and S2, which is about 12% higher than S1 and about 20% higher than S2. Especially in the 6:00~12:00 and 18:00~22:00 periods when the new energy output cannot meet the demand of load growth, the output of traditional energy

units increases, and the output of traditional energy units increases. However, at this point, multi-energy storage devices are also actively responding and taking on some of the regulatory pressure.

The output cost of each peak-shaving unit in the system is shown in Figure 9.

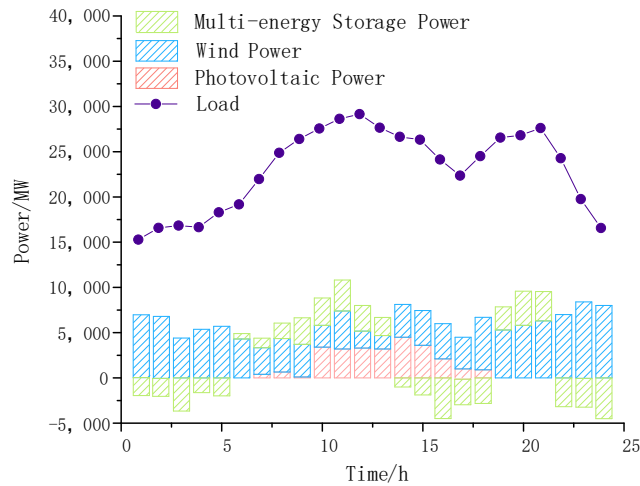


Figure 7. New energy power output optimization under S3.

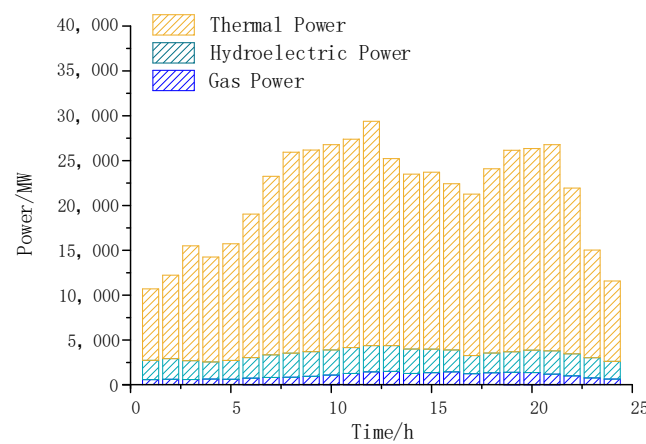


Figure 8. Traditional power unit output under S3.

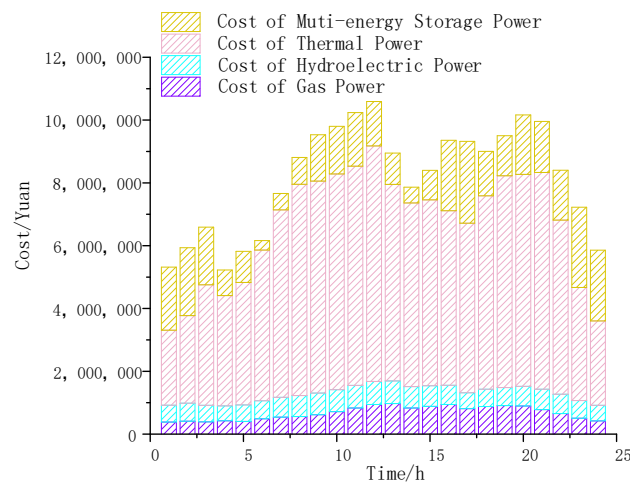


Figure 9. Multi-energy power system peak-shaving cost under S3.

In terms of peak-shaving cost, it can be seen from the comparison between Figures 6 and 9 that the increase in uncertainty of new energy output will inevitably lead to an increase in the reserve capacity of traditional power generation units, thus leading to an increase in the total peak-shaving cost of the system. Especially during peak electricity consumption periods, the additional cost of peak-shaving for thermal power units is relatively high, leading to a significant increase in peak-shaving costs.

### 5.3. Comparison of Optimization Results under Another Solving Algorithm

To verify the superiority of the new energy output optimization algorithm proposed in this article, S4 is set, and different algorithms are used to optimize the new energy output under the same other conditions, and compared with S3.

S4:

When the uncertainty of new energy output is 20%, a multi-objective differential algorithm is used to solve the output optimization of flexible regulating units in the multi-energy system [21], the simulation results are shown in Figures 10 and 11.

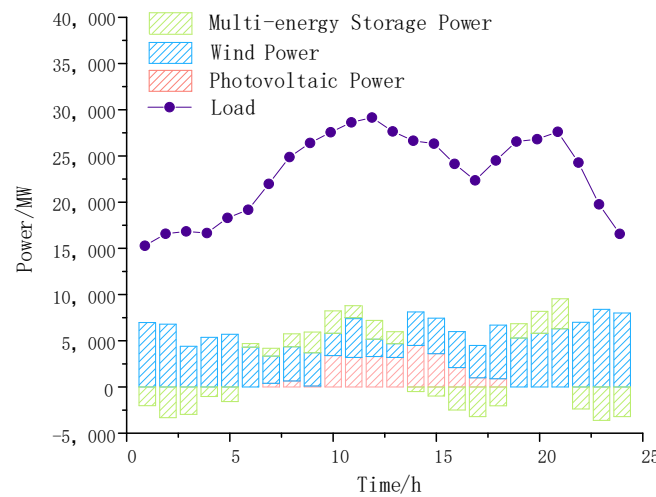


Figure 10. New energy power output optimization under S4.

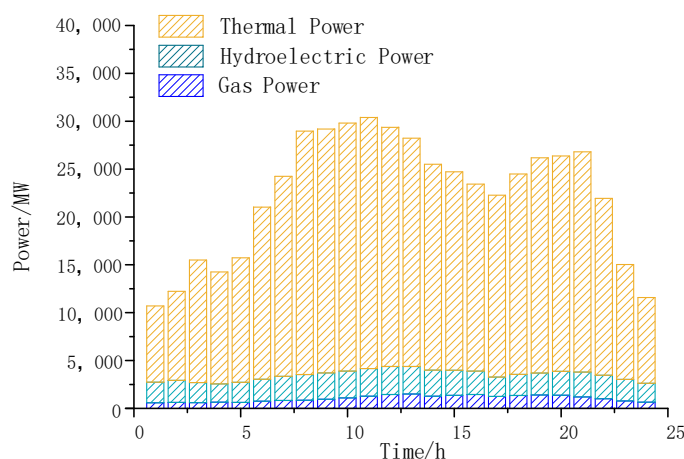
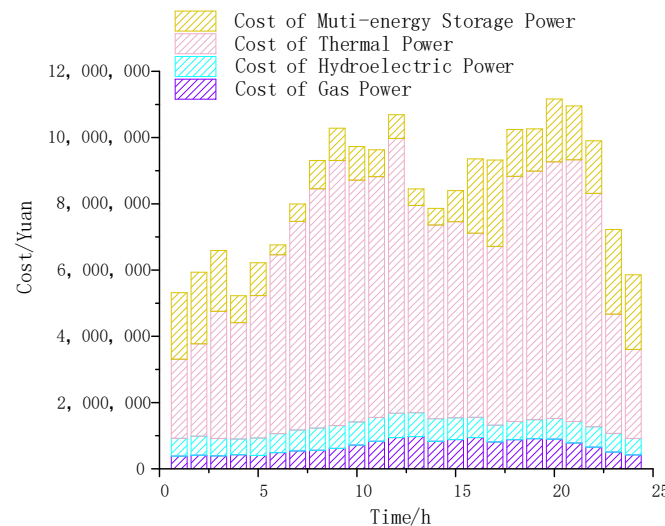


Figure 11. Traditional power unit output under S4.

From Figure 10, it can be seen that compared to Figure 7, the use of a multi-objective differential algorithm for planning multi-source energy storage output results in weaker optimization efforts for new energy output, and the depth of charging and discharging of multi-energy energy storage devices also slightly decreases during low and peak electricity consumption. Therefore, the dynamic optimization algorithm proposed in this article

can better unleash the regulating potential of energy storage devices and achieve a stable output of new energy. As shown in the results in Figure 11, after using the multi-objective differential algorithm for optimization, the reserve capacity of thermal power units has increased compared to Figure 8.

The output cost of each peak-shaving unit in the system is shown in Figure 12.



**Figure 12.** Multi-energy power system peak-shaving cost under S4.

In terms of peak-shaving cost, it can be seen from the comparison between Figures 9 and 12 that due to the high additional cost coefficient of traditional power generation units, multi-energy storage devices that can suppress the uncertainty of new energy output at a lower cost can produce better economic results. Verified the superiority of the dynamic optimization algorithm for new energy output proposed in this article in terms of power regulation and economy.

## 6. Conclusions and Prospects

In response to the strong uncertainty of new energy output in multi-energy systems, this paper proposes a dynamic optimization method for new energy output in multiple time intervals based on the coordination of multiple energy storage devices.

First, a model for energy conversion and regulation characteristics of multi-energy storage devices was studied; then, according to the fluctuation characteristics of new energy output, a dynamic optimization strategy of new energy output based on the time discretization of an output optimization problem is proposed, and the solution model is established; finally, based on the data of the multi-energy system in actual operation, a simulation system was established, and the conclusions of simulation verification are as follows:

- (1) In the process of optimizing new energy output based on multi-energy storage devices, each energy storage device participates in regulation, which can fully unleash the charging and discharging potential of the energy storage device and effectively suppress fluctuations in new energy output.
- (2) The enhancement of uncertainty in the output of new energy will inevitably lead to an increase in the system's peak-shaving pressure and cost. However, using the dynamic optimization algorithm proposed in this article allows multi-energy systems to still provide sufficient load reserve and temporary stable reserve even when traditional power generation units use smaller start-up methods, reducing the system's peak-shaving pressure.

- (3) In terms of peak-shaving costs, the method proposed in this article can suppress the uncertainty of new energy output at a lower cost and improve the operational economy of multi-energy systems.

In summary, the control method proposed in this paper has a good adjustment effect in terms of system power balance and economy; however, there are many calculation steps in the simulation process. Therefore, future research on the simplification of the solution steps and the rate improvement of the algorithm proposed in this paper is a good research direction. Moreover, in the process of new energy stabilization, the different configuration capacities and types of multi-energy storage in the power grid will lead to different stabilization results. Therefore, the optimal configuration scheme of energy storage suitable for the control method proposed in this paper is also one of the future research directions.

**Author Contributions:** This article was written by Q.W., who carried out the design and data analysis of the main research, S.C. led the writing of the article, S.M. and Z.C. gave guidance to the paper. All authors have made contributions to the writing and revision of the article, and have suggestions for improvement to ensure that the article can accurately express complex research results. All authors have read and agreed to the published version of the manuscript.

**Funding:** This research was funded by the National Key Research and Development Program of China (No. 2017YFB0902100).

**Data Availability Statement:** The simulation analysis part of this article is based on real operating power grid data, and for confidentiality reasons, the data in this article will not be disclosed.

**Conflicts of Interest:** The authors declare no conflict of interest.

## References

1. Li, Y.; Zhang, H.; Liang, X.; Huang, B. Event-triggered based distributed cooperative energy management for multi-energy systems. *IEEE Trans. Ind. Inf.* **2019**, *15*, 2008–2022. [[CrossRef](#)]
2. Luo, S.; Peng, K.; Hu, C.; Ma, R. Consensus-Based Distributed Optimal Dispatch of Integrated Energy Microgrid. *Electronics* **2023**, *12*, 1468. [[CrossRef](#)]
3. Gao, F.; Gao, J.; Huang, N.; Wu, H. Optimal Configuration and Scheduling Model of a Multi-Park Integrated Energy System Based on Sustainable Development. *Electronics* **2023**, *12*, 1204. [[CrossRef](#)]
4. Zhang, J.; Li, H.; Li, W.; Zhang, H.; Wang, B. Discussion on the pathways of China's electrification polices to pursue the carbon neutralization target. *Electr. Power Constr.* **2022**, *43*, 47–53.
5. Li, Y.; Gao, D.W.; Gao, W.; Zhang, H.; Zhou, J. Double-Mode Energy Management for Multi-Energy System via Distributed Dynamic Event-Triggered Newton-Raphson Algorithm. *IEEE Trans. Smart Grid* **2020**, *11*, 5339–5356. [[CrossRef](#)]
6. Li, Y.; Gao, D.W.; Gao, W.; Zhang, H.; Zhou, J. A Distributed Double-Newton Descent Algorithm for Cooperative Energy Management of Multiple Energy Bodies in Energy Internet. *IEEE Trans. Ind. Inf.* **2021**, *17*, 5993–6003. [[CrossRef](#)]
7. Jin, H.; Teng, Y.; Zhang, T.; Wang, Z.; Deng, B. A locational Marginal Price-Based Partition Optimal Economic Dispatch Model of Multi-Energy Systems. *Front. Energy Res.* **2021**, *9*, 694983. [[CrossRef](#)]
8. Hu, H.; Sun, X.; Zeng, B.; Gong, D.; Zhang, Y. Enhanced evolutionary multi-objective optimization-based dispatch of coal mine integrated energy system with flexible load. *Appl. Energy* **2022**, *307*, 118130. [[CrossRef](#)]
9. Lei, Y.; Chen, X.; Jiang, K.; Li, H.; Zou, Z. A Novel Methodology for Electric-Thermal Mixed Power Flow Simulation and Transmission Loss Analysis in Multi-Energy Micro-Grids. *Front. Energy Res.* **2021**, *8*, 620259. [[CrossRef](#)]
10. Wei, J.; Zhang, Y.; Wang, J.; Cao, X.; Khan, M.A. Multi-period planning of multi-energy microgrid with multi-type uncertainties using chance constrained information gap decision method. *Appl. Energy* **2020**, *260*, 114188. [[CrossRef](#)]
11. Jiang, Y.; Wan, C.; Chen, C.; Shahidehpour, M.; Song, Y. A Hybrid Stochastic-Interval Operation Strategy for Multi-Energy Microgrids. *IEEE Trans. Smart Grid* **2019**, *11*, 440–456. [[CrossRef](#)]
12. Wang, R.; Sun, Q.; Hu, W.; Li, Y.; Ma, D.; Wang, P. SoC-Based Droop Coefficients Stability Region Analysis of the Battery for Stand-Alone Supply Systems with Constant Power Loads. *IEEE Trans. Power Electron.* **2021**, *36*, 7866–7879. [[CrossRef](#)]
13. Si, F.; Han, Y.; Zhao, Q.; Wang, J. Cost-effective operation of the urban energy system with variable supply and demand via coordination of multi-energy flows. *Energy* **2020**, *203*, 117827. [[CrossRef](#)]
14. Azimi, M.; Salami, A. A new approach on quantification of flexibility index in multi-carrier energy systems towards optimally energy hub management. *Energy* **2021**, *232*, 120973. [[CrossRef](#)]
15. Sun, P.; Teng, Y.; Chen, Z. Robust coordinated optimization for multi-energy systems based on multiple thermal inertia numerical simulation and uncertainty analysis. *Appl. Energy* **2021**, *296*, 116982. [[CrossRef](#)]

16. Feng, L.; Jian, Q.; Tian, H.; Zhao, L.; Liu, R.; Zhao, E. Optimal dispatch and economic evaluation of zero carbon park considering capacity attenuation of shared energy storage. *Electr. Power Constr.* **2022**, *43*, 112–121.
17. Yan, J.; Teng, Y.; Chen, Z. Optimization of Multi-energy Microgrids with Waste Process Capacity for Electricity-hydrogen Charging Services. *CSEE J. Power Energy Syst.* **2021**, *8*, 380–391.
18. Weng, C.; Hu, Z.; Zhang, C.; Li, X.; Wang, F. Distributed planning model of renewable vehicle energy supply station considering seasonal hydrogen storage. *Electr. Power Constr.* **2022**, *43*, 37–46.
19. Shi, Y.; Jin, L.; Li, S.; Li, J.; Qiang, J.; Gerontitis, D.K. Novel Discrete-Time Recurrent Neural Networks Handling Discrete-Form Time-Variant Multi-Augmented Sylvester Matrix Problems and Manipulator Application. *IEEE Trans. Neural Netw. Learn. Syst.* **2022**, *33*, 587–599. [[CrossRef](#)]
20. Mei, J.; Ren, W.; Chen, J. Distributed Consensus of Second-Order Multi-Agent Systems with Heterogeneous Unknown Inertias and Control Gains Under a Directed Graph. *IEEE Trans. Autom. Control* **2015**, *61*, 2019–2034. [[CrossRef](#)]
21. Teng, Y.; Sun, P.; Luo, H.; Chen, Z. Autonomous Optimization Operation Model for Multi-source Microgrid Considering Electrothermal Hybrid Energy Storage. *Proc. CSEE* **2019**, *39*, 5316–5324+5578.

**Disclaimer/Publisher’s Note:** The statements, opinions and data contained in all publications are solely those of the individual author(s) and contributor(s) and not of MDPI and/or the editor(s). MDPI and/or the editor(s) disclaim responsibility for any injury to people or property resulting from any ideas, methods, instructions or products referred to in the content.